Bactericidal activity of amphipathic cationic antimicrobial peptides involves altering the membrane fluidity when interacting with the phospholipid bilayer

Omardien, S.; Drijfhout, J.W.; Vaz, F.M.; Wenzel, M.; Hamoen, L.W.; Zaat, S.A.J.; Brul, S.

DOI
10.1016/j.bbamem.2018.06.004

Publication date
2018

Document Version
Final published version

Published in
Biochimica et Biophysica Acta Biomembranes

BBA - Biomembranes 1860 (2018) 2404–2415

Contents lists available at ScienceDirect

BBA - Biomembranes

journal homepage: www.elsevier.com/locate/bbamem

Bactericidal activity of amphipathic cationic antimicrobial peptides involves altering the membrane fluidity when interacting with the phospholipid bilayer

Soraya Omardien[a], Jan W. Drijfhout[b], Frédéric M. Vaz[c], Michaela Wenzel[d], Leendert W. Hamoen[d], Sebastian A.J. Zaat[e,1], Stanley Brul[a,*,1]

[a] Swammerdam Institute for Life Sciences, Department of Molecular Biology and Microbial Food Safety, University of Amsterdam, Amsterdam, The Netherlands
[b] Leiden University Medical Centre (LUMC), Leiden University, Leiden, The Netherlands
[c] Laboratory Genetic Metabolic Diseases, Academic Medical Centre, Amsterdam, The Netherlands
[d] Swammerdam Institute for Life Sciences, Department of Bacterial Cell Biology and Physiology, University of Amsterdam, Amsterdam, The Netherlands
[e] Department of Medical Microbiology, Amsterdam Infection and Immunity Institute, Academic Medical Centre, University of Amsterdam, Amsterdam, The Netherlands

ARTICLE INFO

Keywords:
Amphipathic cationic antimicrobial peptides
Membrane fluidity
Essential membrane proteins
Bacillus subtilis

ABSTRACT

Background: Amphipathic cationic antimicrobial peptides (AMPs) TC19 and TC84, derived from the major AMPs of human blood platelets, thrombocidins, and Bactericidal Peptide 2 (BP2), a synthetic designer peptide showed to perturb the membrane of *Bacillus subtilis*. We aimed to determine the means by which the three AMPs cause membrane perturbation *in vivo* using *B. subtilis* and to evaluate whether the membrane alterations are dependent on the phospholipid composition of the membrane.
Methods: Physiological analysis was employed using Alexa Fluor 488 labelled TC84, various fluorescence dyes, fluorescent microscopy techniques and structured illumination microscopy.
Results: TC19, TC84 and BP2 created extensive fluidity domains in the membrane that are permeable, thus facilitating the entering of the peptides and the leakage of the cytosol. The direct interaction of the peptides with the bilayer create the fluid domains. The changes caused in the packing of the phospholipids lead to the delocalization of membrane bound proteins, thus contributing to the cell's destruction. The changes made to the membrane appeared to be not dependent on the composition of the phospholipid bilayer.
Conclusions: The distortion caused to the fluidity of the membrane by the AMPs is sufficient to facilitate the entering of the peptides and leakage of the cytosol.
General significance: Here we show *in vivo* that cationic AMPs cause "membrane leaks" at the site of membrane insertion by altering the organization and fluidity of the membrane. Our findings thus contribute to the understanding of the membrane perturbation characteristic of cationic AMPs.

1. Introduction

With the rise of antibiotic resistance, antimicrobial peptides (AMPs) have been proposed as an alternative novel class of antibiotics. Studies seek to understand the mechanism of binding and membrane distortion of AMPs with the intention to improve the design of synthetic or derived peptides. Biophysical studies using model membrane systems are commonly used since biological membranes tend to be multifarious, whereas model membranes can have specifically defined properties. However, it is often in dispute about whether these studies fully explain the complex interaction between AMPs and microbial membranes of living cells. Knowledge of the mode of action of AMPs performed with living microbial cells, to corroborate or to contradict observation made with lipid vesicles, could be beneficial in understanding the membrane perturbation mechanism of AMPs.

"Pore-formation" of cationic peptides is associated with the toroidal model, where the AMP is thought to insert into the membrane causing the membrane to bend inward with the AMP-lipid head groups facing the central pore [1]. The alternative model is the carpet model, where the peptide accumulates at higher concentrations at the cell membrane surface causing the membrane to break off into micelles structures as if treated with a detergent [1,2]. Membrane thinning [3] and phase

* Corresponding author.
E-mail address: s.brul@uva.nl (S. Brul).
[1] Both authors contributed equally.

https://doi.org/10.1016/j.bbamem.2018.06.004
Received 8 November 2017; Received in revised form 5 June 2018; Accepted 6 June 2018
Available online 11 June 2018

boundary defects [4–7] have also been associated with pore-formation. However, instead of viewing pore-formation as a ordered event, it likely should be considered stochastic as proposed in studies performed with alamethicin [8], melittin [9], magainin [10] and maculatin [11]. Recently, the mode of action of lipopeptide daptomycin and the non-pore-forming cyclic hexapeptide cWFW [12,13] was attributed to the altering of membrane fluidity. Here we aimed at extending the analyses on membrane fluidity to our cationic AMPs derived from thrombocidin (TC19 and TC84) and the designer peptide (BP2) that have been shown to perturb the membrane of *B. subtilis* (Omardien, submitted). We expected to see similarities between the TC peptides, and possible differences with BP2. BP2 was characterized previously by a very rapid killing efficacy and hence in that regard a bench-mark for the TC peptides [14].

We found that TC19, TC84 and BP2 altered the fluidity of the membrane of *B. subtilis* vegetative cells. A-typical fluid domains were created within an otherwise rigid membrane. We propose that the distortion of the membrane fluidity leads to "pore-formation", which facilitate the passage of the peptides to the intracellular compartment. Additionally, we found that the activity of TC19, TC84 and BP2 was not necessarily dependent on the composition of the phospholipid bilayer but on the presence of anionic phospholipids, as assessed using phospholipid synthesis mutant *B. subtilis* strains.

2. Materials and methods

2.1. AMP information, strains used and the culturing conditions

Stocks of 1.2 mM TC19 (LRCMCIKWWSGKHPK), TC84 (LRAMCIKWWSGKHPK) and BP2 (GKWKLFKKAFKKFLKILAC) were made in 0.01% acetic acid. Stocks were stored at −20 °C and thawed on ice prior to each experiment. *B. subtilis* pre-cultures were prepared by inoculating a single colony from Luria Broth (LB) solid medium into 5 ml LB liquid medium and culturing overnight. The overnight culture was re-inoculated to have an initial optical density at an absorbance of 600 nm (OD_{600}) of 0.05 in complete minimal medium (CMM) or Luria Broth (LB). CMM consist of Spizizen's Minimal Medium (SMM), as described in Anagnostopoulos & Spizizen (1960) [15], with the modifications described in Halbedel et al. (2014) [16]. The culture was incubated until an OD_{600} of 0.4 to 0.6 (the early exponential growth phase) was reached. Cultures were subsequently diluted for each experiment to an optical density (OD_{600}) of 0.2, if not specified otherwise. Culturing was performed at 37 °C under continuous agitation at 200 rpm where appropriate. Culturing media were supplemented when required as indicated at the specific experiment descriptions. Information about *Bacillus subtilis* strains used in the study and the medium supplements required for each strain can be found in the Table S1. The *Staphylococcus aureus* strain NCTC8325 used in this study was pre-cultured in LB but cultured in CMM.

2.2. Measuring loss of membrane potential using the fluorescent probe $DiSC_3(5)$

To determine the loss of membrane potential after treatment with the AMPs the fluorescent dye *3,3′-dipropylthiadicarbocyanine iodide* ($DiSC_3(5)$) was used. The method was followed as described in Breeuwer & Abee [17] with some alterations. In brief, 200 µl diluted pre-cultures of *B. subtilis* were added to each well in a 96-well flat-bottomed microtiter plate (µClear, polystyrene, black wall, clear bottom, Greiner Bio-One). $DiSC_3(5)$ was added to each well to have a final concentration of 1.5 µM. Cells with an active membrane potential will accumulate the dye in their membrane, reducing the $DiSC_3(5)$ signal. Once the $DiSC_3(5)$ signal had reduced to close to zero, the AMPs were added. Loss of membrane potential will cause release of the dye again. As positive controls for membrane potential loss, valinomycin (Sigma-Aldrich) was added at a final concentration of 30 µM, and Nisin A (> 95% purity; Handary, Belgium) at a final concentration of 4 µM. To a sample of untreated cells 1% DMSO was added to assess the total fluorescence of the dye taken up prior to initiation of treatment. Following treatment of the cells with the AMPs, additional valinomycin was added at a final concentration of 30 µM to dissipate the residual membrane potential. The assay was performed at 37 °C while shaking. Fluorescence was measured at an excitation wavelength of 622 nm and emission wavelength of 670 nm, with the BioTek Synergy Mx, Gen5 2.0 (Winooski, VT) plate reader. Three biological repeats were performed.

2.3. Labelling procedure of peptide TC84 using Alexa Fluor 488

For solid phase peptide synthesis, the chemical procedures were followed as described by Heimstra et al. [18]. The amino acid sequence of TC84 was N-terminally elongated with a cysteine residue to enable coupling of the Alexa Fluor 488. The internal cysteine residue was protected during synthesis with an acid-stable StBu group, resulting in the intermediate peptide C- L- R- A- M- C(StBu)- I- K- W- W- S- G- K- H- P- K-amide. The intermediate peptide (18 mg in 1 ml DMSO) was added to Alexafluor488 C-5 maleimide (20 mg in 1 ml DMSO, A10254, Life Technologies). To this solution 1 µl 4-methylmorpholine (NMM) was added. The resulting mixture was vortexed for 10 s and left at room temperature for 40 min. The reaction was stopped by the addition of 500 µl acetic acid/water at a 9:1 ratio. The labelled product was purified by reversed phase chromatography on a C18-column using water to acetonitrile gradient containing 0.1% TFA, and lyophilized. The StBu protected labelled peptide obtained was dissolved in 300 µl water/acetonitrile at a 1:1 ratio and treated with ten-fold excess TCEP (TCEP·HCl was neutralised with 4 N NaOH) for 3 h at room temperature to remove the StBu protection. After lyophilisation and desalting on a PD-10 column using water/acetonitrile/acid at a 40:60:10 ratio as an eluent, the final product was obtained (Microflex, Bruker). Quantification was performed by OD_{495} using an ε of 71,000. The labelled peptide was stored at −20 °C until further use.

2.4. Laurdan staining to observe changes in membrane fluidity after the addition of peptides

Changes in membrane fluidity were observed using Laurdan (6-Dodecanoyl-*N*, *N*-dimethyl-2-naphthylamine; Sigma Aldrich), a fluorescent probe sensitive to membrane phase transitions. For Laurdan staining of *B. subtilis* cells, the method described by H. Strahl et al. [19] was followed with minor alterations. The culture was incubated until an OD_{600} of 0.4 to 0.6 was reached in CMM or LB. Laurdan, dissolved in dimethylformamide (DMF), was added at a final concentration of 10 µM. The mixture was incubated for an additional 5 min at 37 °C while shaking in the dark. Stained cells were washed (four times for spectroscopy measurements and twice for microscopy) and re-suspended in PBS buffer (PBS containing 0.2% w/v glucose and 1% v/v DMF). The stained cells were diluted to an OD_{600} of 0.2 before the addition of AMPs. Laurdan stained cells were washed only once after staining for treatment with Alexa 488-labelled TC84. After Alexa 488-labelled TC84 treatment, cells were subsequently washed four times and re-suspended with pre-warmed PBS buffer.

Laurdan fluorescence spectroscopy measurements were performed by adding to each well of a 96-well flat-bottomed microtiter plate (µClear, polystyrene, black wall, clear bottom, Greiner Bio-One) stained cells with AMPs to have a final volume of 200 µl. Fluorescence was measured in a BioTek Synergy Mx, Gen5 2.0 (Winooski, VT) plate reader every 2 min while shaking at 37 °C. After 4 min of measuring, AMPs were added and additional measurements were taken for 30 min. Laurdan was measured at an excitation wavelength of 350 nm and the emission wavelength at 460 ± 5 nm ((liquid ordered or gel-phase; g) and 500 ± 5 nm ((liquid disordered or liquid-phase; l). Laurdan generalized polarization (GP) was calculated using the formula Laurdan $GP = (I_g - I_l) / (I_g + I_l)$, where I_g is the fluorescent measurement in the

gel-phase and I_l the fluorescent measurement in the liquid-phase. The culture was maintained at 37 °C throughout the assay.

Laurdan microscopy measurements were performed by treating stained cells for 5 min with the AMPs before visualizing the Laurdan using a temperature-controlled Nikon Eclipse Ti fluorescence microscope. Laurdan was excited at a wavelength of 340–380 nm and emission were at 435–485 nm (gel-phase) and 510–560 nm (liquid-phase). Laurdan GP of the microscopy images were performed using the CalculateGP ImageJ plugin designed by Norbert Vischer (https://sils.fnwi.uva.nl/bcb/objectj/examples/CalculateGP/MD/gp.html).

2.5. $DiIC_{12}$ staining to confirm fluid regions in membrane after peptide treatment

$DiIC_{12}$ is a short chain cationic lipophilic fluorescent probe that preferentially partitions into areas in the bilayer that is in fluid-phase (liquid disordered phase) [20]. Cells were stained before treatment by culturing *B. subtilis* or *S. aureus* in CMM or LB containing 1 μg/ml $DiIC_{12}$ (dissolved in DMSO) until an OD_{600} of 0.2 to 0.6 was reached. Stained cells were diluted to an OD_{600} of 0.2 if necessary with CMM or LB containing 1% v/v DMSO. Stained cells were washed four times with medium and subsequently treated with AMPs for 5 min. The culture was maintained at 37 °C throughout the assay. Cells were visualized with a Cy3 filter using a temperature-controlled Nikon Eclipse Ti fluorescence microscope.

2.6. Structure illumination microscopy (SIM) imaging of membrane after peptide treatments

The *B. subtilis* PrpsD-sfGFP mutant constitutively produces the green fluorescent protein under control of the promotor for ribosomal protein S4 and was used to observe membrane perturbation and cytosol leakage. Diluted pre-cultures of *B. subtilis* PrpsD-sfGFP were treated with the AMPs for 5 min. AMP-treated cells were stained with Nile Red (0.5 μg/ml final concentration). The culture was maintained at 37 °C throughout the assay. The Nikon N-SIM E microscope was used to visualize the cells. The coverslips were coated with L-dopamine to reduce the binding of Nile Red in order to avoid distortion of the structured illumination pattern projections [21,22].

2.7. Determining the binding site of peptide TC84 using Alexa-488 labelled TC84

Pre-cultures of *B. subtilis* were washed once and re-suspended in phosphate buffer saline (PBS, pH 7.4) containing 0.2% w/v glucose. The suspensions were diluted to an OD_{600} of 0.2 with PBS with 0.2% w/v glucose prior to treatment with 14 μM Alexa 488-labelled TC84. Combination treatments of Alexa 488-labelled TC84 and active TC84 at a 1:1 w/w mixture, to have a final concentration of 14 μM were also performed. Treatments were for 5 min followed by two washing steps with PBS with 0.2% w/v glucose to remove residual labelled peptide. To determine whether the Alexa 488-labelled TC84 delocalize membrane bound proteins, *B. subtilis* mutants producing the peripheral membrane bound protein MreB (MreB-mCherry) and integral membrane bound protein PBP2b (PBP2b-mCherry) fused to the fluorescent protein, mCherry, were used. Treatment of the *B. subtilis* mutants were similar as mentioned above. The culture was maintained at 37 °C throughout the assay. Fluorescence microscopy imaging with the Nikon Elipse Ti was performed at an excitation wavelength and emission wavelength for mCherry (570 ± 10 nm/620 ± 10 nm) and Alexa 488-labelled TC84 (490 nm ± 5 nm/525 nm ± 5 nm). Labelling of TC84 with Alexa Fluor 488 reduced the efficacy of the peptide up to 56 μM, the highest concentration tested.

2.8. Killing efficacy of peptides using mutants with an altered membrane phospholipid composition

B. subtilis mutants were cultured in CMM containing the necessary supplements for each strain (Table S1). In short, *B. subtilis* strain MHB001 (*pgsA*) was cultured with erythromycin and isopropyl β-D-1-thiogalactopyranoside (IPTG) at a final concentration of 1 mM or 0.1 mM to induce *pgsA* expression. *B. subtilis* strain HB5337 (*mprF*) was cultured with kanamycin, HB5362 (*ywnE*) with chloramphenicol and strain SDB206 (CL) with spectinomycin. Diluted pre-cultures were treated with the AMPs for 30 min. Aliquots were taken and diluted as mentioned in the time-kill assay. The culture was maintained at 37 °C throughout the assay. Results were expressed as numbers of CFU/ml. Four biological repeats were performed. Statistical analysis was performed in SigmaPlot 13.0.

2.9. Software and fluorescence microscopes employed in the study

Microscopy images were analysed in ImageJ/Fiji (http://rbsweb.nih.gov/ij/). Microscopy imaging was performed using the Nikon Eclipse Ti equipped with an Intensilight HG 130 W lamp, a C11440-22CU Hamamatsu ORCA camera, a CFI Plan Apochromat DM 100× oil objective and OkoLab stage incubator (Napoli, Italy). Structured illumination microscopy (SIM) was performed with a Nikon Ti N-SIM equipped with a CFI SR Apochromat TIRF 100× oil objective (NA1.49), a LU-N3-SIM laser unit, an Orca-Flash 4.0 sCMOS camera (Hamamatsu Photonics K·K). Software used for the Nikon Elipse Ti was the NIS elements software version 4.20.01 and for the SIM reconstruction was NIS-elements Ar software.

3. Results

3.1. TC19, TC84 and BP2 dissipate the membrane potential gradually

Previously, it was observed that TC-1, the original protein design template for TC19 and TC84, did not dissipate the membrane potential of *Lactococcus lactis* [23]. Recently, lipopeptide daptomycin was shown to cause a gradual membrane dissipation profile compared to the K^+/Na^+ channel-forming Gramicidin ABCD peptide mix, as detected using the fluorescent dye $DiSC_3(5)$ [12]. We employed $DiSC_3(5)$ to evaluate whether TC19, TC84 and BP2 dissipate the membrane potential rapidly as expected with pore-forming peptides. The positively charged $DiSC_3(5)$ accumulates intracellularly during hyperpolarization of the membrane and is released from the cell when depolarization takes place [24]. A loss of $DiSC_3(5)$ signal is observed after the addition of the dye due to its spectral shift once it is aggregated intracellularly. When the ionophore valinomycin is added, it dissipates the membrane potential in the presence of potassium ions, resulting in a rapid increase in the $DiSC_3(5)$ signal [25]. The lantibiotic Nisin A was added as a control. Nisin binds to lipid II, a membrane-anchored cell wall precursor that is essential for cell wall biosynthesis, to form defined pores [26].

Valinomycin instantly dissipated the membrane potential (Fig. 1). Peptide TC84, TC19 and BP2 dissipated the membrane potential (Fig. 1), but with lethal concentration of TC19 (14 μM), TC84 (14 μM) and BP2 (3.5 μM) (Omardien, submitted) only a gradual increase in $DiSC_3(5)$ signal was observed. A "lag time" of about 5 min was required before an increase in $DiSC_3(5)$ could be observed. Only after about 25 min of treatment with TC19 and TC84 did the $DiSC_3(5)$ signal reach its maximum, suggesting a slow depolarization of the membrane. The delayed increase in $DiSC_3(5)$ signal of TC19 and TC84 was similar to what was observed for the lipopeptide daptomycin [12], but differed from pore-forming lantibiotic Nisin A, the K^+/Na^+ channel-forming peptide mix Gramicidin ABCD [12] and the helical pore-forming peptide KLA-1 [13]. A delay in $DiSC_3(5)$ signal was also observed for Nisin A compared to valinomycin, but the delay was shorter than for TC19 and TC84 (Fig. 1). BP2 caused a similar $DiSC_3(5)$ signal profile as Nisin

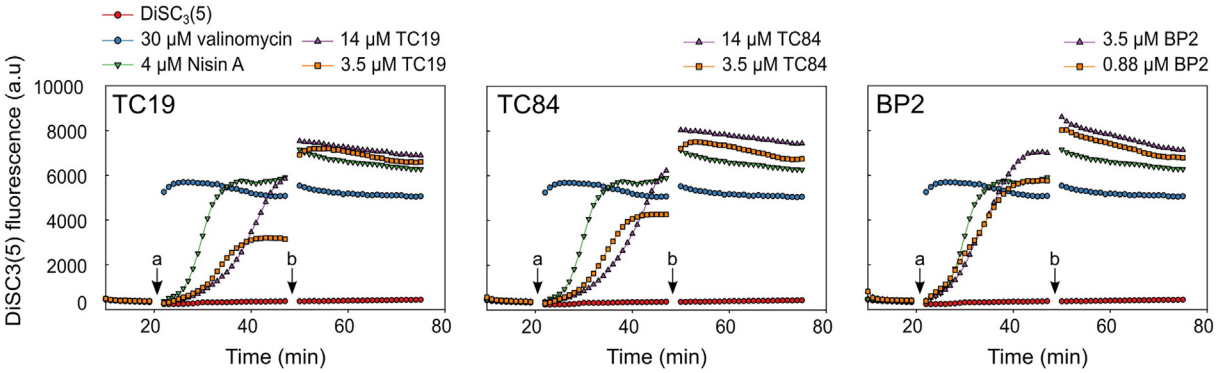

Fig. 1. Graphs depicting the loss of membrane potential after treatment with TC19, TC84, BP2, Nisin A and valinomycin using the fluorescent dye $DiSC_3(5)$. After the addition of $DiSC_3(5)$, the dye accumulates within the cell deploying its membrane potential. a) Valinomycin, TC19, TC84, BP2 and Nisin A was added 10 min after the addition of $DiSC_3(5)$. Valinomycin rapidly dissipates the membrane potential ($\Delta\Psi$) in the presence of potassium ions. TC19, TC84, BP2 and the control Nisin A dissipated the membrane potential, but slower than valinomycin. b) Additional valinomycin was added 25 min after the addition of the peptides to completely dissipate the membrane potential. Results are expressed at relative fluorescence in arbitrary units (a.u).

A. Additional valinomycin was added after 30 min of treatment with the AMPs and a further increase in $DiSC_3(5)$ release was observed suggesting that complete dissipation of the membrane potential does not occur after treatment with TC19, TC84 and BP2. A further increase in $DiSC_3(5)$ release was not observed for valinomycin. Valinomycin functions as a potassium ion carrier that specifically dissipates the membrane potential in the presence of potassium ions [25], thus increasing the concentration of valinomycin in the medium will not cause further loss in membrane potential. In conclusion, these data led us to infer that TC19 and TC84 might cause changes to the fluidity to the membrane similar to what has been seen for daptomycin [12].

3.2. TC19, TC84 and BP2 distort the membrane by creating fluid membrane domains

To evaluate whether our AMPs affect membrane fluidity the fluorescent probe Laurdan was employed. Laurdan localizes at the hydrophobic-hydrophilic interface of the phospholipid bilayer where the lauric acid tail of this fluorescent probe is anchored in the phospholipid acyl chain region [27]. In the gel phase (liquid ordered) phospholipids are tightly packed and less water molecules are present than in the loosely packed liquid-phase (liquid disordered) [27–29]. Upon excitation, the dipolar moment of Laurdan is influenced by the dipolar moment of surrounding water molecules causing a spectral shift. Thus, Laurdan anchored in a gel-phase (blue) will emit at a different wavelength compared to when the compound is present in a liquid membrane-phase (red). We found that culturing *B. subtilis* in CMM (defined minimal medium) resulted in a smaller cell size compared to *B. subtilis* cells obtained from rich LB medium cultures. Furthermore, previous studies made use of *B. subtilis* cultured in LB to evaluate changes in membrane fluidity using Laurdan [12,13]. Hence to cover both minimal and rich environmental conditions, we decided to study *B. subtilis* cells obtained from both CMM and LB cultures when evaluating membrane alterations.

TC19, TC84 and BP2 caused a rapid increase in Laurdan general polarization (GP) values, suggesting an instant membrane rigidification (< 2 min) after the addition of the peptides (Fig. 2A). The negative controls treated with the solvent used for the peptides showed no change in membrane fluidity, whereas benzyl alcohol (BA) rapidly fluidized the membrane as expected. BA increases the penetration of water molecules into the hydrophobic region of the phospholipid bilayer thus increasing the liquid-phase of the membrane [19,30]. Similarly, daptomycin and the non-pore-forming cyclic hexapeptide cWFW showed to cause rapid membrane rigidification, and it was suggested that the changes in fluidity are due to direct insertion of these agents into the membrane [12,13].

Laurdan fluorescence microscopy images were evaluated for *B. subtilis* cells cultured in CMM (Fig. 2B). However, *B. subtilis* cells cultured in CMM was too small to visualize the effect of the peptides on the membrane, therefore changes in membrane fluidity were evaluated using LB cultured cells (Fig. 3A). The images confirmed the increase in fluidity of BA treated cells compared to untreated cells (Fig. 3A and B). After treatment with TC19, TC84 and BP2 the images revealed large liquid-phase domains in the membrane, but an increase in gel-phase of the membrane bulk (Fig. 3A and B). Staining with $DiIC_{12}$, confirmed the formation of fluid domains in the membrane after treatment with the AMPs (Fig. 4). $DiIC_{12}$ differs from Laurdan in that it preferentially partitions out of the gel-phase into the liquid-phase [20,31]. $DiIC_{12}$ was also employed to observe whether changes in the membrane fluidity will arise when treating the pathogenic *Staphylococcus aureus* (Fig. 4). We also included the membrane permealizing lantibiotic Nisin A [26] and alpha-helical peptide LL-37 [32]. We found, similar to *B. subtilis*, the presence of fluid domains in the membrane after treatment with TC19, TC84 and BP2, but also with LL-37 and Nisin A.

To confirm the observed alteration to the membrane and cytosol leakage, *B. subtilis* PrpsD-sfGFP stained with the membrane dye, Nile Red, were evaluated using SIM after treatment with lethal concentrations of TC19, TC84 or BP2. Nile Red has a stronger signal when the membrane is in fluid phase. Untreated cells showed equal distribution of Nile Red fluorescence over the membrane. After treatment, *B. subtilis* PrpsD-sfGFP showed perturbed membrane domains characterized by unequal staining near the septum, but also at random areas in the membrane similar to what was observed with the Laurdan GP images (Fig. 5). These observations suggest that plasmolysis occurs when lethal concentrations are used. The perturbed membrane areas were curved inwards and the Nile Red signal appeared more intense at these perturbed membrane areas compared to the rest of the membrane, suggesting that these areas were more fluid than the rest (Fig. 5). Less PrpsD-sfGFP signal was also observed at the perturbed membrane areas.

3.3. Confirmation of membrane alterations using an Alexa Fluor 488 labelled TC84

To observe the possible binding site of the AMPs, TC84 was employed as a reference peptide and labelled with Alexa Fluor 488. Labelling of TC84 with Alexa Fluor 488 altered the activity of the peptide as the MIC value was higher than the highest tested concentration of 56 μM (Fig. S1). At 56 μM Alexa Fluor 488 labelled TC84 (Alexa488-TC84) we did observe an extended lag time of the cell growth in the culture in comparison with the growth kinetics observed in cultures exposed to lower Alexa488-TC84 concentrations. Fifty-six micromolar Alexa488-TC84 reduced the culture by one log CFU/ml

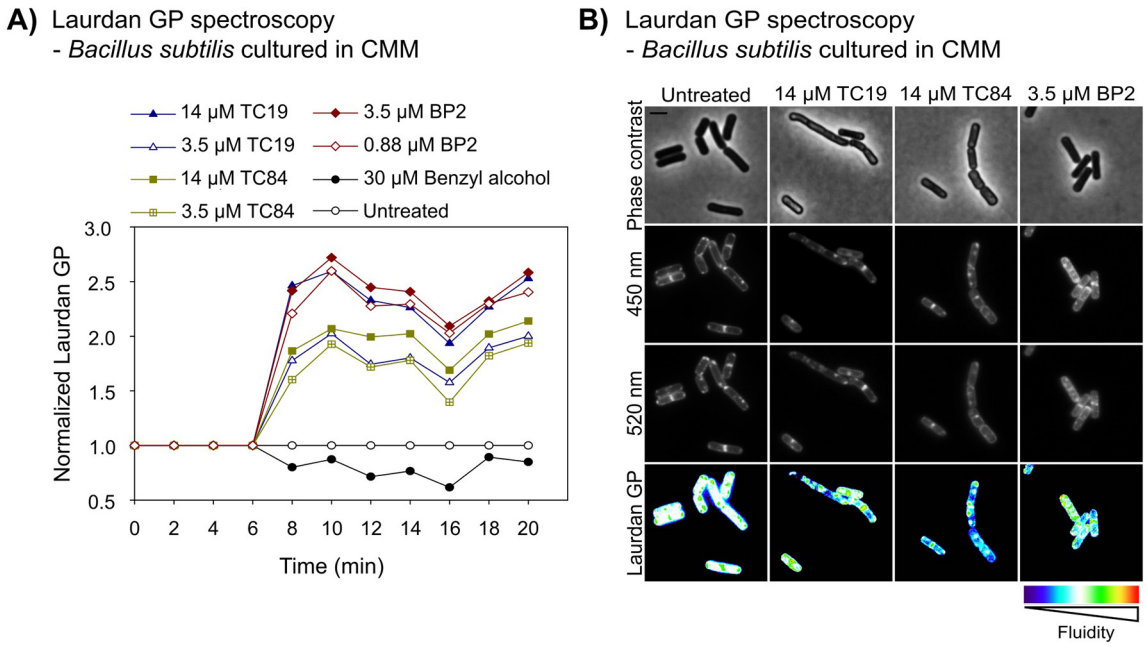

Fig. 2. Laurdan staining of *B. subtilis* after peptide treatment to determine membrane fluidity alterations. (A) Spectroscopy measurements showed the rapid rigidification of the membrane after the addition of TC19, TC84 and BP2 with an increase in Laurdan GP values compared to the untreated cells. Benzyl alcohol, a known membrane fluidizer, indeed increased membrane fluidity with a Laurdan GP value lowered compared to that of untreated cells. Laurdan GP values were normalized against those of untreated cells. Fluorescence microscopy images showed that TC19, TC84 and BP2, after 5 min of treatment, create fluid domains in the membrane of *B. subtilis* cultured in CMM. Scale bar represent 2 µm.

after 15 min of treatment, possibly causing the lag time in the growth curve observed. We hypothesize that the anionic bulky Alexa Fluor 488 moiety reduces the electrostatic interaction required for cationic TC84 to interact with the anionic cell envelope of *B. subtilis*. A reduction in antimicrobial activity of magainin 2, PGLa [34] and daptomycin [12] was also observed after fluorophore labelling. Nevertheless, in the case of the labelled magainin 2 and PGL the desired synergism was observed as with the unlabelled peptides. Also, exposure of cells to fluorescently labelled daptomycin lead to a similar phenotype as was observed after incubation of *B. subtilis* cells with the unlabelled peptide. In summary, results obtained with labelled peptides, including our Alexa488-TC84, should be interpreted with caution. The data should only be used as a proxy for the understanding of the mechanistic details of the mode of action of the parent peptides. Alexa488-TC84 at 14 µM bound rapidly (≤ 5 min) to the membrane. The fluorescent compound accumulated at the septum, but also at lower intensity at random areas of the membrane (Fig. 6B). Anionic phospholipid CL were previously reported to be located at the septum and poles of *B. subtilis* membranes [35], suggesting that the peptides interact with this anionic phospholipid. However, the location of CL are currently in dispute [36]. Moreover, the Alexa488-TC84 binding sites co-localized with the fluid domains observed in the co-staining Laurdan GP images. The binding of Alexa488-TC84 to the cell membrane was irreversible as the peptide remained bound after multiple washing steps. These finding suggested that TC84 might also bind to and remain within the phospholipid bilayer of the cell membrane. Laurdan stained cells were treated with 14 µM Alexa488-TC84 for 5 min to evaluate whether fluid domains are formed. Indeed, Alexa488-TC84 was bound to fluidic areas (Fig. 6B). These finding suggest that the fluid domains observed are formed at sites of accumulation of the peptides in the membrane. We hypothesize that the insertion of the peptides into the membrane locally increases the concentration of water molecules and the mobility of the acyl chains. The presence of the rigid bulk membrane, however, is unclear. The fluorescent probe $DiIC_{12}$ has been shown to preferentially partition into fluid domains, as reported by Baumgart et al. [20]. We pre-stained our cells with DiIC12 before treatment with the peptides and found $DiIC_{12}$ to accumulate in regions that are most likely in liquid-phase (liquid disordered) (Fig. 4.). There is a possibility that the phospholipids (unsaturated or branched) associated with liquid disordered regions are removed from the bulk membrane and accumulate in the observed fluid domains. However, this is a speculation, and we know of no method to determine the characteristics of phospholipids locally in the membrane.

Similar to situation with unlabelled TC84, the change in fluidity induced by the insertion of Alexa488-TC84 into the membrane caused the peripheral membrane protein MreB (MreB-mCherry) and the integral membrane protein PBP2b (PBP2b-mCherry) to delocalize (Fig. 6C). Cells treated with the low concentration of 14 µM Alexa488-TC84 had membrane invaginations where the peptide was bound (Fig. 6D). At a high concentration of 56 µM Alexa488-TC84, an invaginated membrane with co-localizing peptide was also observed and the peptide accumulated intracellularly. Combining Alexa488-TC84 with unlabelled TC84, which has a much higher antimicrobial activity, also showed that the Alexa488-TC84 accumulate intracellularly (Fig. 6E), suggesting that the membrane perturbation caused by the AMPs might facilitate the entering of the peptides into the cells.

3.4. Membrane alterations in B. subtilis phospholipid synthesis mutants are insufficient to prevent the AMPs' activity

The membrane has been shown to be the primary target of TC19, TC84 and BP2. Therefore, we questioned whether the activity of the peptides is dependent on the composition of the phospholipid bilayer of the *B. subtilis* cell membrane. The general consensus is that cationic antimicrobial peptides are attracted to the bacterial cell surface through electrostatic interaction. This is considered to be due to the cationic nature of the peptide and the anionic surface charge of the cell envelope [37]. This hypothesis is supported by the notion that modifications of the anionic PG reducing the net negative surface charge of the bacteria, also reduce the efficacy of antimicrobial peptides. For example, lysylation of PG resulted in reduction in susceptibility of *Staphylococcus aureus* to antimicrobial peptides [38–44]. Lysyl-PG was also shown to

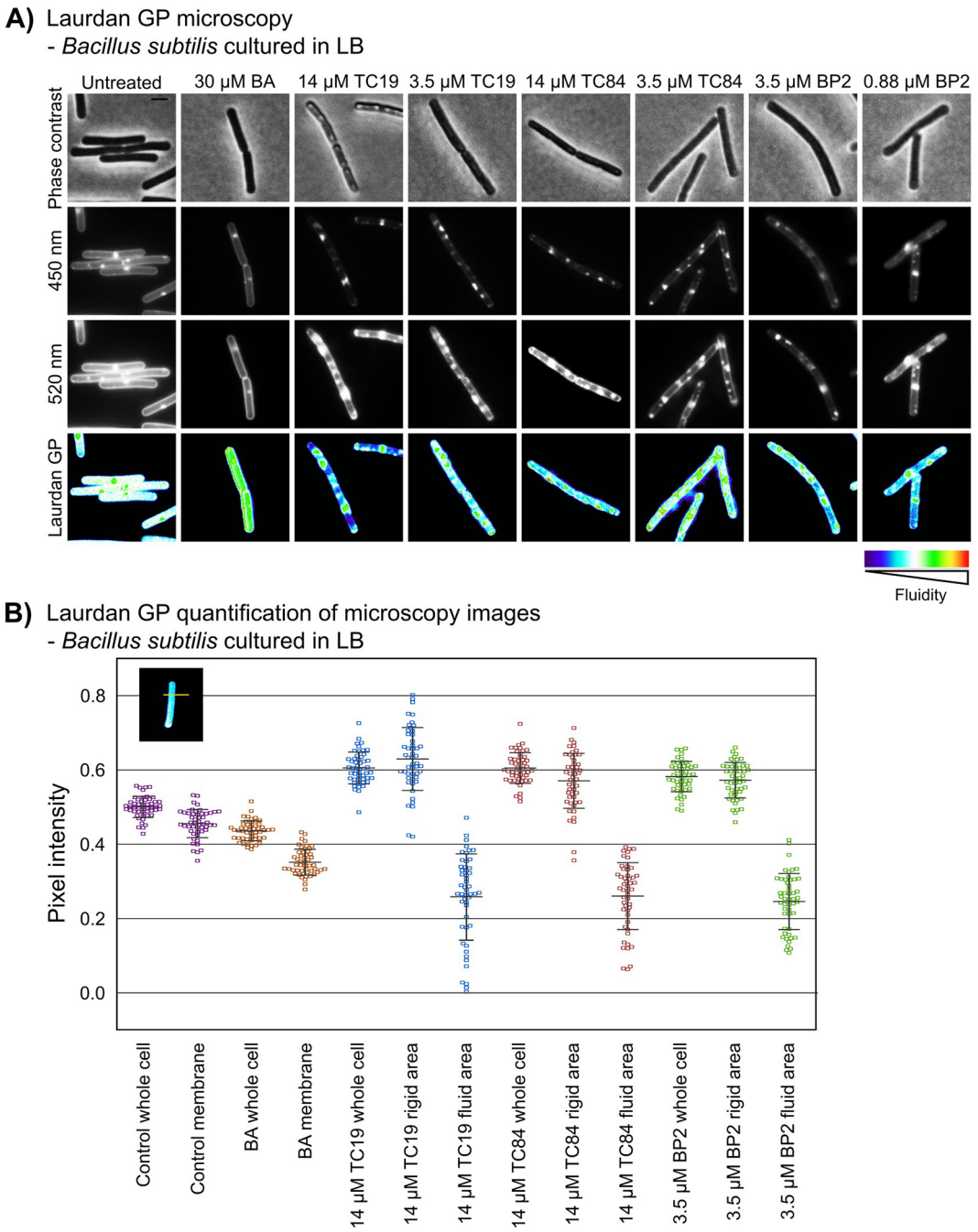

Fig. 3. Laurdan staining of *B. subtilis* after peptide treatment to determine membrane fluidity alterations. (A) Fluorescence microscopy images showed that TC19, TC84 and BP2, after 5 min of treatment, create fluid domains in the membrane of *B. subtilis* cultured in LB. The rest of the membrane was more rigid. (D) Quantification of pixel intensity showed that the fluid domains were more fluid and the rigid areas were more rigid than in the untreated cells. Scale bar represent 2 μm.

be important for *B. subtilis* peptide resistance when a loss of function of MprF caused an increase in sensitivity to Nisin [45]. The activity of daptomycin were also affected by the presence of PG and lysyl-PG in the membrane [46–49].

The phospholipids that contribute to the negative charge of the membrane are PG, cardiolipins (CL) and lysyl-PG. PgsA, phosphatidylglycerophosphate synthase, catalyzes PG formation [45]. Cardiolopin synthases YwnE, YwjE and YwiE condense two PG molecules to form CL [35,45]. MprF, lysyl-phosphatidylglycerol synthase, transfers a lysyl group to PG forming lysyl-PG thus reducing the negative charge of the phospholipid [45]. To assess the role of these phospholipids in TC19, TC84 and BP2 susceptibility, four mutants with altered phospholipid composition were used. *B. subtilis* strain MHB001, referred to as 1A700-PgsA, has the essential gene *pgsA* replaced by the IPTG inducible P*spac-pgsA* [50]. *B. subtilis* strain HB5337 (referred to as CU1065-MprF) has the non-essential gene *mprF* deleted [45]. *B. subtilis* strain HB5362 (referred to as CU1065-YwnE) has the *ywnE* (*clsA*) gene deleted, which encodes the major cardiolipin synthase [45]. *B. subtilis* strain SDB206 (referred to as 168-CL) had all three cardiolipin synthases *ywnE*, *ywjE* and *ywiE* deleted, and should have hardly any CL [35].

Lipidomic analyses were performed of the *B. subtilis* strains to confirm the expected changes to the phospholipid composition of the mutants. The membrane of the CU1065-MprF strain had lysyl-PG

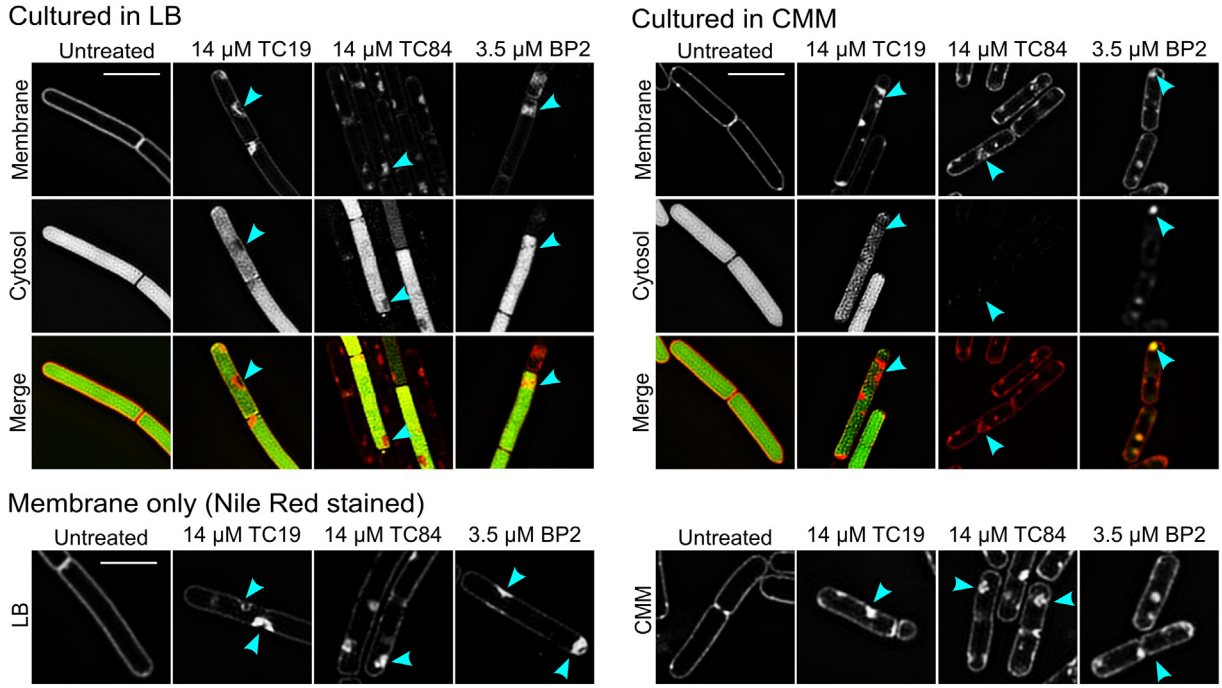

Fig. 4. Fluorescence microscopy images of $DiIC_{12}$ stained *B. subtilis* and *S. aureus* to confirm changes in membrane fluidity after treatment with TC19, TC84 and BP2. After 5 min of treatment of *B. subtilis* cells, fluid membrane domains were observed similar to those observed in Laurdan stained cells (Fig. 2 and 3). Fluid lipid domains are clearly visible after treatment with all three peptides in *B. subtilis* cells cultured in LB and CMM. After 5 min of treatment of *S. aureus* cells, fluid lipid domains were also clearly visible in the membrane. The membrane active alpha-helical peptide LL-37 also caused the formation of fluid domains in the membrane *S. aureus*. Lantibiotic Nisin A also showed changes in the fluidity of the membrane after treatment.

decreased, PE increased, and PG and CL at similar levels compared to the wild type CU1065 (Fig. 7). The results confirm that the content of the positively charged phospholipid lysyl-PG in the membrane is reduced. The CU1065-MprF strain, however, was not more sensitive to TC19, TC84 and BP2 as compared to the wild type CU1065 (Fig. 7), implying that lowering lysyl-PG in the membrane does not have an effect on the susceptibility for these AMPs.

The CU1065-YwnE strain had CL and PE reduced in the membrane compared to the wild type CU1065 (Fig. S1). Similar to the CU1065-YwnE strain, the 168-CL strain had CL and PE reduced without a clear

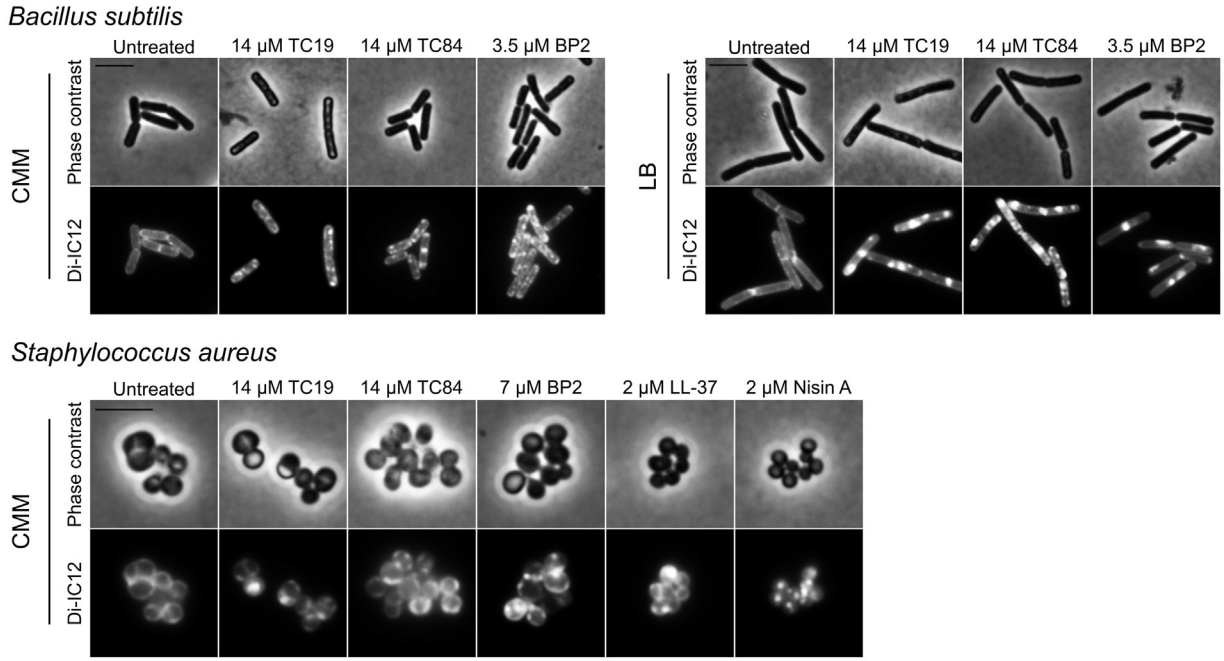

Fig. 5. Structured illumination microscopy (SIM) imaging of *B. subtilis* PrpsD-sfGFP after peptide treatment. *B. subtilis* PrpsD-sfGFP cultured in LB and CMM after treatment with lethal concentrations of TC19 (14 μM), TC84 (14 μM) and BP2 (3.5 μM) to probe for membrane deformation and possible cytosolic leakage. The membrane was stained with Nile red. LB and CMM cultured cells showed deformed membrane areas at the cell poles and septum, but also at random locations on the membrane (turquois arrows). Leakage of the cytosol was observed with the loss of PrpsD-sfGFP signal, but membrane deformation did not always cause cytosol leakage. Scale bar represents 2 μm.

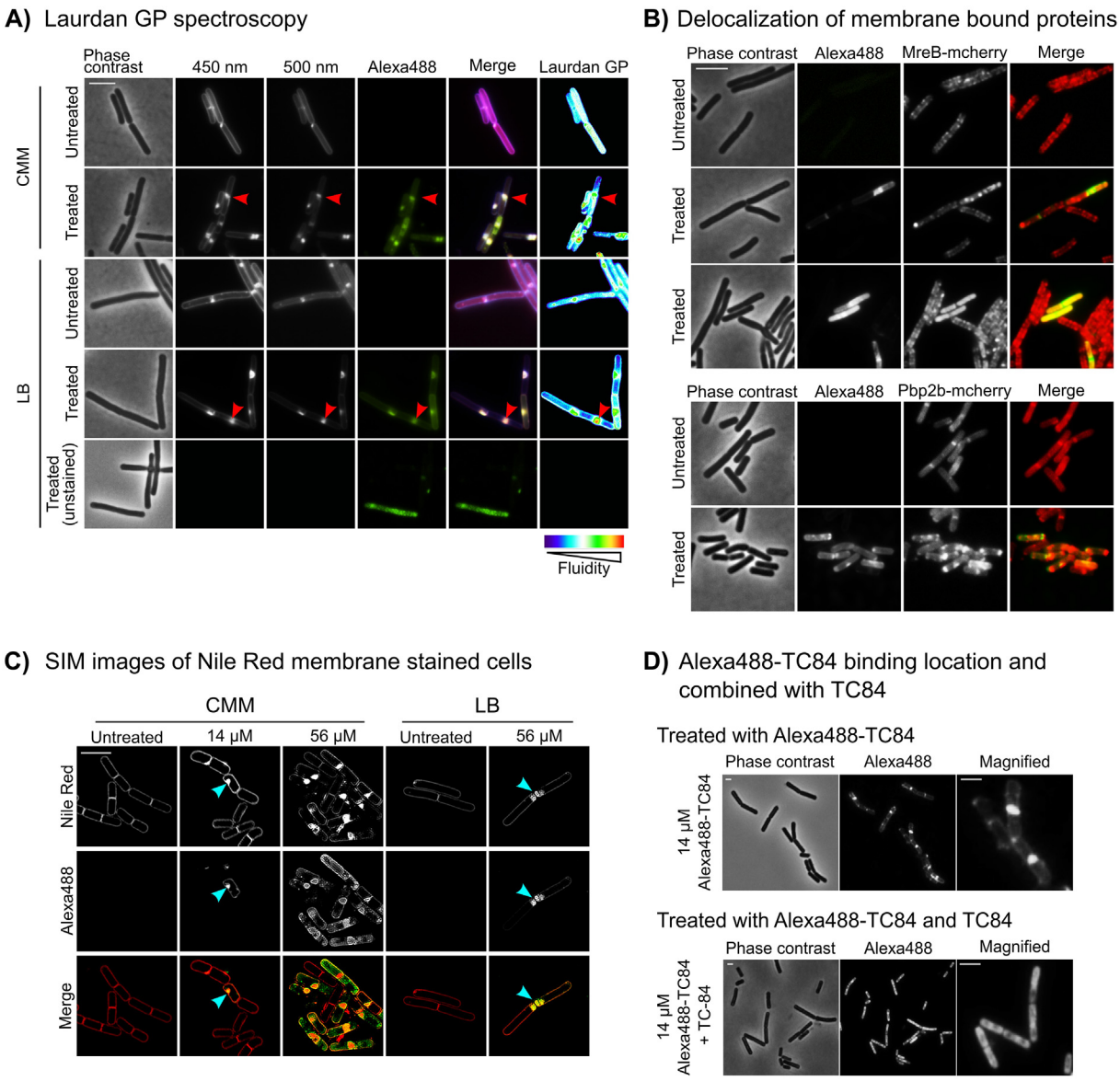

Fig. 6. Assessment of possible binding sites of TC84 using Alexa Fluor 488. (A) Laurdan stained cell were treated with Alexa488-TC84 to observed changes in membrane fluidity. The accumulation of Alexa488-TC84 overlapped with the location of the fluid domains (red arrows). (B) Treatment of *B. subtilis* mutants with the peripheral membrane protein MreB (MreB-mCherry) and integral membrane protein PBP2b (PBP2b-mCherry) fused to the mCherry red fluorescent protein. MreB-mCherry and PBP2b-mCherry were delocalized after treatment. Delocalized PBP2b-mCherry did not co-localize with Alexa488-TC84 (turquoise arrows). (C) SIM images of Nile Red stained *B. subtilis* treated with Alexa488-TC84. (D) Alexa488-TC84 combined with TC84 in a 1:1 ratio (final concentration of 14 µM). All treatments were for 5 min and cells were washed with phosphate buffered saline (PBS) after treatment. Scale bar represent 2 µm.

change in lysyl-PG content in the membrane (Fig. S1). The PG (32:0), PG (32:0) [M + OH] −, PG (33:1), PG (34:0), PG (34:0) [M + OH] − and PG (35:0) content, however, appeared to have increased suggesting that the reduction in CL might be compensated for by increasing the PG content. Furthermore, PG will not be converted to CL due to the lack of cardiolipin synthases. The reduced CL and PE content of the membrane did not decrease the efficacy of the AMPs (Fig. 7), suggesting that CL and PE are not essential for the membrane activity of the AMPs. The presence of PG and possibly the increase of the different PG species, might be sufficient for the AMPs to interact with the membrane.

Strain 1A700-PgsA cultured in the presence of 1 mM IPTG had an increase in PE, PG (31:1) and PG (32:1) without a clear change in lysyl PG or CL compared to the wild type 1A700 (Fig. S2). The net effect on the overall membrane charge might be negligible. Changes to the 1A700-PgsA strain cultured in the presence of 0.1 mM IPTG were more complex. The strain had an increase in cytidine diphosphate diacylglycerol (CDPDG), and a reduction in CL and PG. However, PG (31:1), PG (32:1), PG (34:0), PG (34:1) and PG (35:0) were increased in the membrane. An increase of about 40% PE and 30% lysyl-PG, of the total PE and lysyl-PG, were also observed. The combined effect of these changes on the net charge of the membrane is difficult to predict. Strain 1A700-PgsA cultured in 1 mM IPTG or 0.1 mM IPTG was not more nor less sensitive compared to the wild type 1A700 to the activity of the AMPs (Fig. 7). In conclusion, these results show that changes in lipid composition due to particular mutations are not necessarily entirely predictable and suggest that changes in phospholipid composition of the membrane mentioned above are not essential in determining the AMPs efficacy.

4. Discussion

In this study, we aimed to determine the membrane perturbation

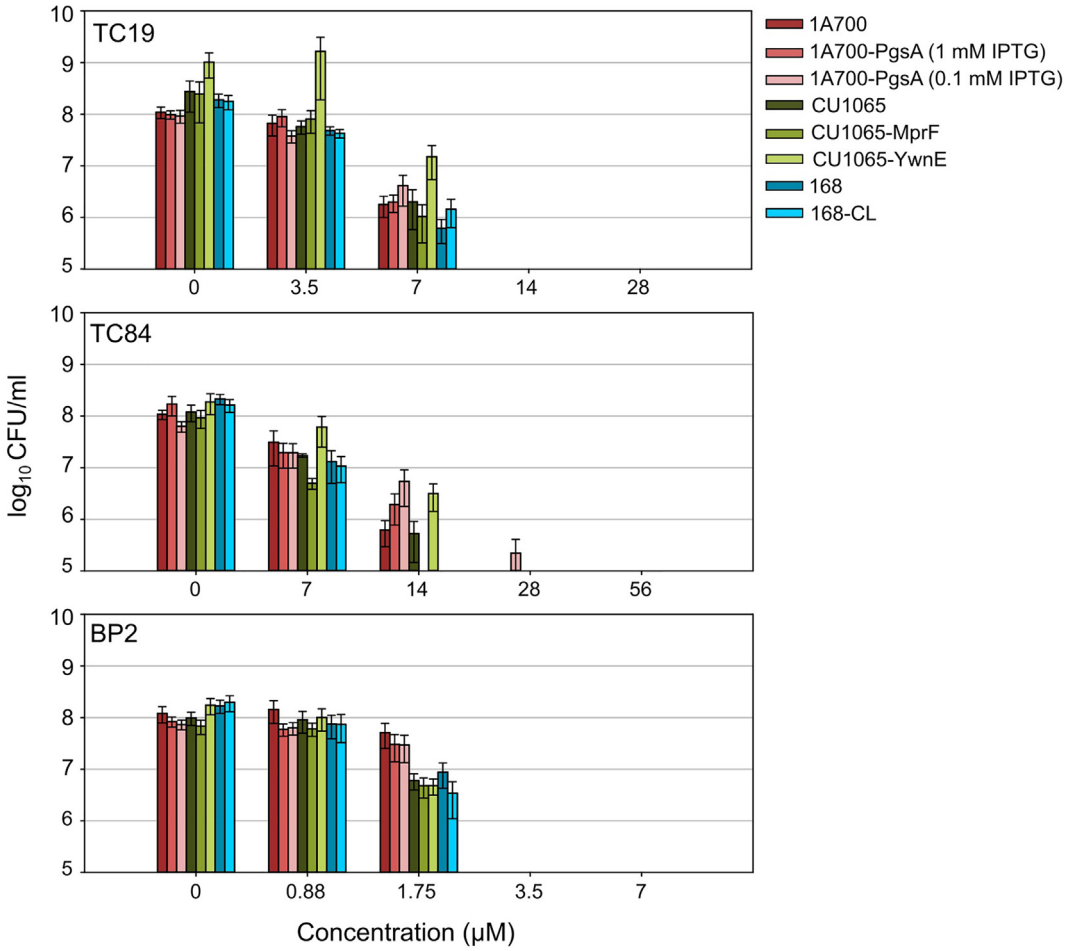

Fig. 7. The survival of *B. subtilis* wild type and membrane phospholipid mutant strains after peptide treatment. The susceptibility of wild type strains *B. subtilis* 1A700 was compared with that of a *B. subtilis pgsA* conditional mutant (strain 1A700-PgsA) cultured at 1 mM and 0.1 mM IPTG (the minimal IPTG level compatible with strain viability). The survival of a *B. subtilis mprF* deletion mutant (strain CU1065-MprF) lacking lysyl-phosphatidylglycerol (lysyl-PG) and a *B. subtilis ywnE* deletion mutant (strain CU1065-YwnE) lacking cardiolopin (CL) was compared with survival of wild type *B. subtilis* CU1065. Wild type strain 168 was compared with triple cardiolipin synthase deletion mutant (strain 168-CL). No significant differences in susceptibility to TC19, TC84 and BP2 were observed between the mutant strains and their wild type. Treatment with TC19, TC84 and BP2 was for 30 min. Standard error bars represent four biological repeats.

mechanism of amphipathic cationic AMPs derived from thrombocidin, TC19 and TC84, and designer peptide BP2. TC19 and TC84 dissipated the membrane potential gradually, whereas BP2 dissipated the membrane potential faster than TC19 and TC84. The $DiSC_3(5)$ profiles of TC19 and TC84 were similar to what was observed for lipopeptide daptomycin [12] but different from the instant membrane dissipation profile of the K^+/Na^+ channel-forming peptide mix Gramicidin ABCD [12], the helical pore-forming peptide KLA-1 [13] and Nisin in our study. Daptomycin was shown to significantly perturb the membrane without permeabilising it, by inserting into regions of increased fluidity (RIFs) [12]. We hypothesized that our amphipathic cationic AMPs, TC19, TC84 and BP2, would alter membrane fluidity similar to daptomycin. Unlike daptomycin, TC19, TC84 and BP2 caused rapid membrane permeabilisation without causing overt cell lysis, as observed with the TEM and Sytox Green staining images (Omardien, submitted). Daptomycin has shown with $DiIC_{12}$ staining to cause domains in *B. subtilis* membranes after only 10 min of treatment, which were enlarged after 60 min of treatment [12]. These thin domains appeared rigid with Laurdan staining due to the combination of daptomycin and lipids (dapto-lipids) that reduced the mobility of the phospholipids [12]. TC19, TC84 and BP2, however, caused formation of large, clearly defined fluid domains (with Laurdan and $DiIC_{12}$), while the rest of the membrane appeared rigid after 5 min of treatment. The observation that similar fluid domains co-localized with Alexa488-labelled TC84, suggest that it is the interaction of TC19, TC84 and BP2 with the phospholipid bilayer that creates these fluid domains. Fluid domains were also observed in the $DiIC_{12}$ stained membrane of *S. aureus* when treated with TC19, TC84, BP2, the lantibiotic Nisin A and alpha-helical peptide LL-37. Phase boundary defects caused by the phase separation of lipids (Epand et al., 2006, 2008; Epand and Epand, 2009; Jean-François et al., 2008) or membrane thinning [3] have been proposed as a means of compromising the membrane barrier by peptides. We have showed that TC19, TC84 and BP2 causes essential membrane bound proteins to delocalize (Omardien, submitted). Alexa488-labelled TC84 also showed to cause delocalization of peripheral membrane protein MreB (MreB-mCherry) and integral membrane protein PBP2b (PBP2b-mCherry). Peripheral membrane protein MreB has shown to delocalize due to a loss of membrane potential [33], but the integral membrane protein PBP2b has not shown to be sensitive to changes in the membrane potential. We assume that the changes in packing of the phospholipids in the bilayer also contributes to the delocalization of these essential proteins.

The Nile Red staining of peptide-treated cells showed that the peptides cause membrane invagination which indicates plasmolysis. The fluid domains and membrane invaginations co-localized. Staining with Alexa-TC84 confirmed that membrane invagination occurs where the peptide accumulates. The irregular localization of ATP synthase subunit AtpA fused to the green fluorescent protein (GFP) upon

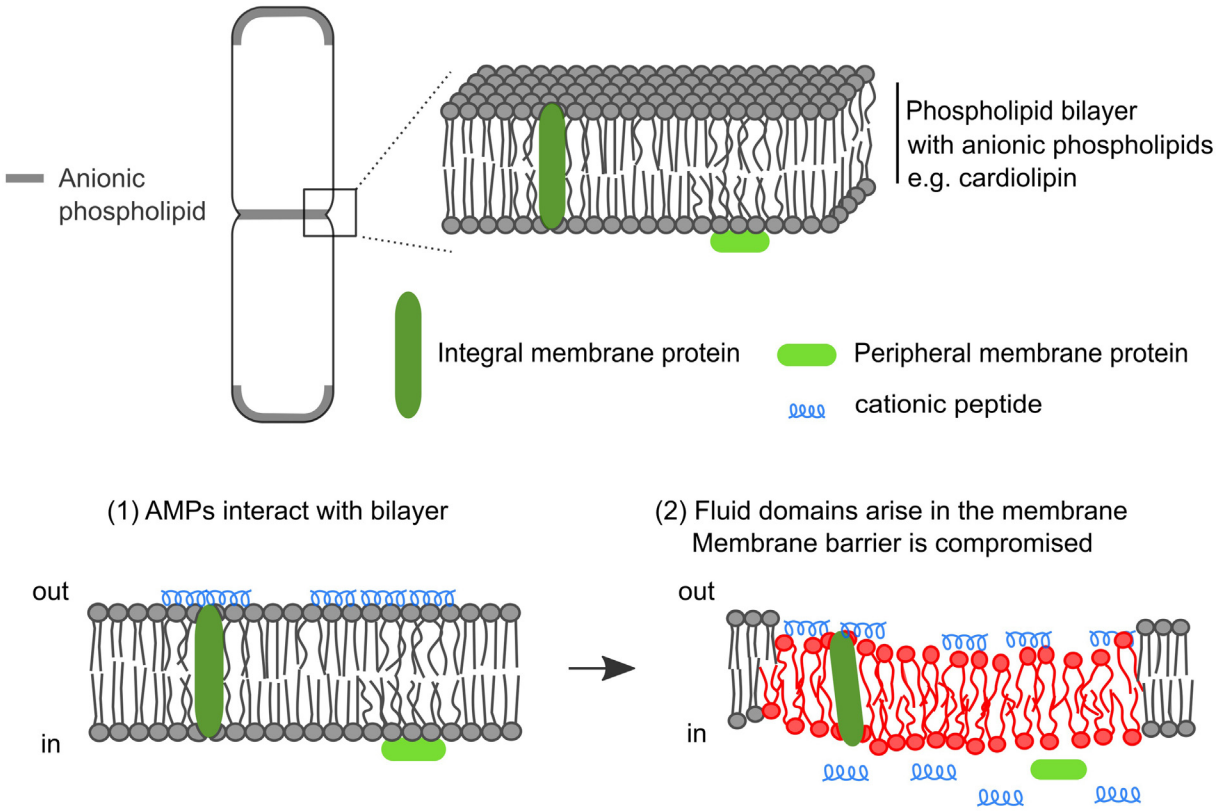

Fig. 8. Model of the effects of TC19, TC84 and BP2 on membrane of *B. subtilis*. (1) The AMPs align on the surface of the membrane. The cationic AMPs have a higher affinity for the anionic phospholipids and therefore accumulate at areas on the membrane associated with these anionic phospholipids such as phosphatidylglycerol and cardiolipin. (2) In *in vitro* studies with artificial membranes, both the insertion and the alignment of the AMPs in parallel to the membrane have been suggested to cause "free volume" in the bilayer [3]. The "free volume" is compensated for which leads to membrane thinning and an increase in fluidity of the hydrophobic core. This phenomenon can contribute to an increase of the liquid disordered area (fluid domains) of the membrane. Changes in the membrane homeostasis cause the delocalization of essential membrane bound proteins. Eventually, leakage of the cytosol and entering of the AMPs into the cell occurs.

treatment with TC19, TC84 and BP2 (Omardien, submitted) also confirms membrane invagination. The irregular distribution of AtpA has been used previously as an indicator for abnormal membrane curvatures [19]. Interestingly, in contrast to our peptides, daptomycin had no effect on the localization of AtpA suggesting that no abnormal membrane curvatures occurs [12] and even though cyclic hexapeptide cWFC altered the localization of AtpA it appeared different from TC19, TC84 and BP2 treated cells (Omardien, submitted). AtpA-GFP was absent from the rigid domains caused by cWFC [13], whereas TC19, TC84 and BP2 causes "patchy" localization of AtpA-GFP. Alexa488-TC84 when used at a high concentration and when combined with TC84 was found intracellularly after treatment, suggesting that TC84 and probably TC19 and BP2 accumulate intracellularly after the membrane barriers is compromised. This suggests that the targeting of intracellular anionic macromolecular components might also be part of the mechanism of killing the cells.

To determine whether the membrane deformations caused by the peptides are dependent on the composition of the membrane, we examined the effects of TC19, TC84 and BP on various *B. subtilis* mutants with altered membrane compositions. The cyclic hexapeptide cWFW *in vitro* caused de-mixing of PG/PE bilayers [51,52], but *in vivo* showed not to be dependent on the PE and CL content of the membrane to create rigid membrane domains [13]. It was proposed that cWFW creates a phase separation by changing the physical state of the membrane and not by inducing the cellular enrichment for a specific phospholipid [13]. Likewise, in our study we did not observe changes in efficacy of TC19, TC84 and BP2 against *B. subtilis* mutants with altered membrane compositions, including mutants with reduced membrane PE and CL content. The *B. subtilis* mutant SDB206 (168-CL) used in the study for cWFW was expected to have no CL present in the cell membrane [13], but in our lipidomic analysis *B. subtilis* mutant SDB206 showed to have PG in the membrane even though the PE and CL content was reduced. We concluded that in absence of CL the essential anionic PG might compensate for this phospholipid, enabling the interaction of the peptides with the membrane that leads to phase boundary defects [4,7]. The cationic phospholipid lysyl-PG has been implicated in the resistance of Gram-positives against cationic antimicrobial peptides as it is thought to reduce the net negative surface charge of the membrane, reducing the electrostatic interaction with the cationic peptides. We did however not observe a reduced sensitivity to TC19, TC84 and BP2 for the *B. subtilis* mutants with reduced lysyl-PG (strain CU1065-MprF) content, suggesting that altering the overall surface charge of the phospholipid bilayer of the cells might not be sufficient to prevent the activity of these AMPs. However, we did not address the effects of modifying the cell wall, such as D-alanylation of the teichoic acids, or thickening of the cell wall. These cell wall and cell membrane modification have previously shown to contribute to resisting AMPs by Gram-positives such as *Staphylococcus aureus*, *Enterococcus faecalis* and *Clostridium difficile*; reviewed in Omardien et al., 2016 [53].

4.1. Model of the interaction of TC19, TC84 and BP2 with the membrane

We hypothesize that the cationic residues (arginine, histidine and lysine) of TC19, TC84 and BP2 interact with the anionic phospholipids of the bacterial membrane bilayer. The anionic phospholipids are CL and PG [54], but the membrane sites of these phospholipids are unclear and in dispute [36]. Interaction of the cationic peptide with the anionic

head-groups of the phospholipids will coalesce the phospholipids, thus increasing the free space in the bilayer. The AMPs might be aligning in parallel to the membrane or insert into the upper layer of the phospholipid bilayer, but the nature of the peptide's interaction with the membrane is still unclear (Fig. 8). However, the contact of the AMPs with the phospholipid bilayer causes fluid domains to occur, but we hypothesize that the initial change in membrane fluidity does not cause cell death. In studies with phospholipid vesicles leakage due to a packing defect in the bilayer has been shown in case of a shift in the environmental temperature [55], where this does not lead to cell death. Peripheral membrane proteins are displaced from the membrane, while integral membrane proteins likely remain membrane bound but are misplaced relative to their normal location. We think that a phase boundary defect eventually occurs between the fluid (liquid disordered) and gel (liquid ordered) membrane areas compromising the membrane barrier and increasing the permeability of the membrane. The inability of the bacterial cell to prevent the unfavourable changes to the membrane eventually manifest as membrane inward curvature putatively causing perturbation of the normal membrane physiology and hence favouring the observed gradual dissipation of the membrane potential, internalization of the peptides and leakage of the cytosol.

In conclusion, we show *in vivo* that the cationic peptides, TC19, TC84 and BP2, compromise the membrane barrier by altering the distribution of fluid and rigid areas of the membrane by creating fluid domains (“pores”).

Competing financial interest statement

The authors have no competing interests to declare.

Transparency document

The Transparency document associated with this article can be found in the online version.

Acknowledgements

The authors acknowledge Edward A. de Koning and Terrens N.V. Saaki for constructing the strains EKB154 and TNVS205, and Kate Feller for contributing to Fig. 6 during her Bachelor's internship. S. Omardien acknowledges the Erasmus Mundus Action 2 program (EMA2) and University of Amsterdam for funding. S.A.J. Zaat is supported by the FP7-HEALTH-2011 grant 278890, BALI – Biofilm Alliance. The authors declare that they have no conflict of interest.

Appendix A. Supplementary data

Supplementary data to this article can be found online at https://doi.org/10.1016/j.bbamem.2018.06.004.

References

[1] K.A. Brogden, Antimicrobial peptides: pore formers or metabolic inhibitors in bacteria? Nat. Rev. Microbiol. 3 (2005) 238–250, http://dx.doi.org/10.1038/nrmicro1098.
[2] L.T. Nguyen, E.F. Haney, H.J. Vogel, The expanding scope of antimicrobial peptide structures and their modes of action, Trends Biotechnol. 29 (2011) 464–472, http://dx.doi.org/10.1016/j.tibtech.2011.05.001.
[3] K. Lohner, New strategies for novel antibiotics: peptides targeting bacterial cell membranes, Gen. Physiol. Biophys. 28 (2009) 105–116, http://dx.doi.org/10.4149/gpb_2009_02_105.
[4] R.M. Epand, R.F. Epand, Lipid domains in bacterial membranes and the action of antimicrobial agents, Biochim. Biophys. Acta Biomembr. 1788 (2009) 289–294, http://dx.doi.org/10.1016/j.bbamem.2008.08.023.
[5] F. Jean-François, S. Castano, B. Desbat, B. Odaert, M. Roux, M.H. Metz-Boutigue, E.J. Dufourc, Aggregation of cateslytin β-sheets on negatively charged lipids promotes rigid membrane domains. A new mode of action for antimicrobial peptides? Biochemistry 47 (2008) 6394–6402, http://dx.doi.org/10.1021/bi800448h.
[6] R.F. Epand, M.A. Schmitt, S.H. Gellman, R.M. Epand, Role of membrane lipids in the mechanism of bacterial species selective toxicity by two α/β-antimicrobial peptides, Biochim. Biophys. Acta Biomembr. 1758 (2006) 1343–1350, http://dx.doi.org/10.1016/j.bbamem.2006.01.018.
[7] R.F. Epand, B.P. Mowery, S.E. Lee, S.S. Stahl, R.I. Lehrer, S.H. Gellman, R.M. Epand, Dual mechanism of bacterial lethality for a cationic sequence-random copolymer that mimics host-defense antimicrobial peptides, J. Mol. Biol. 379 (2008) 38–50, http://dx.doi.org/10.1016/j.jmb.2008.03.047.
[8] L. Thøgersen, B. Schiøtt, T. Vosegaard, N.C. Nielsen, E. Tajkhorshid, Peptide aggregation and pore formation in a lipid bilayer: a combined coarse-grained and all atom molecular dynamics study, Biophys. J. 95 (2008) 4337–4347, http://dx.doi.org/10.1529/biophysj.108.133330.
[9] D. Sengupta, H. Leontiadou, A.E. Mark, S.J. Marrink, Toroidal pores formed by antimicrobial peptides show significant disorder, Biochim. Biophys. Acta Biomembr. 1778 (2008) 2308–2317, http://dx.doi.org/10.1016/j.bbamem.2008.06.007.
[10] H. Leontiadou, A.E. Mark, S.J. Marrink, Antimicrobial peptides in action, J. Am. Chem. Soc. 128 (2006) 12156–12161, http://dx.doi.org/10.1021/ja062927q.
[11] D.L. Parton, E.V. Akhmatskaya, M.S.P. Sansom, Multiscale simulations of the antimicrobial peptide maculatin 1.1: water permeation through disordered aggregates, J. Phys. Chem. B 116 (2012) 8485–8493, http://dx.doi.org/10.1021/jp212358y.
[12] A. Müller, M. Wenzel, H. Strahl, F. Grein, T. Saaki, B. Kohl, T. Siersma, J. Bandow, H. Sahl, T. Schneider, L. Hamoen, Daptomycin inhibits bacterial cell envelope synthesis by interfering with fluid membrane microdomains, Proc. Natl. Acad. Sci. U. S. A. 113 (2016) E7077–E7086, http://dx.doi.org/10.1073/pnas.1611173113.
[13] K. Scheinpflug, M. Wenzel, O. Krylova, J.E. Bandow, M. Dathe, H. Strahl, Antimicrobial peptide cWFW kills by combining lipid phase separation with autolysis, Sci. Rep. 7 (2017) 44332, , http://dx.doi.org/10.1038/srep44332.
[14] P.H.S. Kwakman, A.a. Te Velde, C.M.J.E. Vandenbroucke-Grauls, S.J.H. van Deventer, S.A.J. Zaat, Treatment and prevention of Staphylococcus epidermidis experimental biomaterial-associated infection by bactericidal peptide 2, Antimicrob. Agents Chemother. 50 (2006) 3977–3983, http://dx.doi.org/10.1128/AAC.00575-06.
[15] C. Anagnostopoulos, J. Spizizen, Requirements for transformation in *Bacillus subtilis*, J. Bacteriol. 81 (1961) 741–746.
[16] S. Halbedel, M. Kawai, R. Breitling, L.W. Hamoen, SecA is required for membrane targeting of the cell division protein DivIVA in vivo, Front. Microbiol. 5 (2014) 58, , http://dx.doi.org/10.3389/fmicb.2014.00058.
[17] P. Breeuwer, T. Abee, Assessment of the membrane potential, intracellular pH and respiration of bacteria employing fluorescence techniques, Mol. Microbiol. Ecol. Man, Second Ed, Kluwer Academic Publishers, Netherlands, 2004, pp. 3465–3481, , http://dx.doi.org/10.1007/978-1-4020-2177-0_801.
[18] H.S. Hiemstra, G. Duinkerken, W.E. Benckhuijsen, R. Amons, R.R.P. de Vries, B.O. Roep, J.W. Drijfhout, The identification of CD4+ T cell epitopes with dedicated synthetic peptide libraries, Proc. Natl. Acad. Sci. 94 (1997) 10313–10318, http://dx.doi.org/10.1073/pnas.94.19.10313.
[19] H. Strahl, F. Bürmann, L.W. Hamoen, The actin homologue MreB organizes the bacterial cell membrane, Nat. Commun. 5 (2014) 3442, , http://dx.doi.org/10.1038/ncomms4442.
[20] T. Baumgart, G. Hunt, E.R. Farkas, W.W. Webb, G.W. Feigenson, Fluorescence probe partitioning between Lo/Ld phases in lipid membranes, Biochim. Biophys. Acta Biomembr. 1768 (2007) 2182–2194, http://dx.doi.org/10.1016/j.bbamem.2007.05.012.
[21] W. Zhang, F.K. Yang, Y. Han, R. Gaikwad, Z. Leonenko, B. Zhao, Surface and tribological behaviors of the bioinspired polydopamine thin films under dry and wet conditions, Biomacromolecules 14 (2013) 394–405, http://dx.doi.org/10.1021/bm3015768.
[22] H. Strahl, S. Ronneau, B.S. González, D. Klutsch, C. Schaffner-Barbero, L.W. Hamoen, Transmembrane protein sorting driven by membrane curvature, Nat. Commun. 6 (2015) 8728, , http://dx.doi.org/10.1038/ncomms9728.
[23] J. Krijgsveld, S.A.J. Zaat, J. Meeldijk, P.A. van Veelen, G. Fang, B. Poolman, E. Brandt, J.E. Ehlert, A.J. Kuijpers, G.H.M. Engbers, J. Feijen, J. Dankert, Thrombocidins, microbicidal proteins from human blood platelets, are C-terminal deletion products of CXC chemokines, J. Biol. Chem. 275 (2000) 20374–20381, http://dx.doi.org/10.1074/jbc.275.27.20374.
[24] M. Síp, P. Herman, J. Plásek, V. Hrouda, Transmembrane potential measurement with carbocyanine dye diS-C3-(5): fast fluorescence decay studies, J. Photochem. Photobiol. B 4 (1990) 321–328, http://dx.doi.org/10.1016/1011-1344(90)85037-W.
[25] H.M. Shapiro, Cell membrane potential analysis, Methods Mol. Biol, 1994, pp. 121–133, , http://dx.doi.org/10.1016/S0091-679X(08)61713-6.
[26] I. Wiedemann, R. Benz, H.G. Sahl, Lipid II-mediated pore formation by the peptide antibiotic nisin: a black lipid membrane study, J. Bacteriol. 186 (2004) 3259–3261, http://dx.doi.org/10.1128/JB.186.10.3259-3261.2004.
[27] T. Parasassi, G. de Stasio, G. Ravagnan, R.M. Rusch, E. Gratton, Quantitation of lipid phases in phospholipid vesicles by the generalized polarization of Laurdan fluorescence, Biophys. J. 60 (1991) 179–189, http://dx.doi.org/10.1016/S0006-3495(91)82041-0.
[28] T. Parasassi, E. Gratton, Membrane lipid domains and dynamics as detected by Laurdan fluorescence, J. Fluoresc. 5 (1995) 59–69, http://dx.doi.org/10.1007/BF00718783.
[29] T. Parasassi, G. de Stasio, A. D'Ubaldo, E. Gratton, Phase fluctuation in phospholipid membranes revealed by Laurdan fluorescence, Biophys. J. 57 (1990) 1179–1186, http://dx.doi.org/10.1016/S0006-3495(90)82637-0.
[30] I. Konopásek, K. Strzalka, J. Svobodová, Cold shock in *Bacillus subtilis*: different effects of benzyl alcohol and ethanol on the membrane organisation and cell adaptation, Biochim. Biophys. Acta Biomembr. 1464 (2000) 18–26, http://dx.doi.

org/10.1016/S0005-2736(99)00240-0.
[31] J. Zhao, J. Wu, S.L. Veatch, Adhesion stabilizes robust lipid heterogeneity in supercritical membranes at physiological temperature, Biophys. J. 104 (2013) 825–834, http://dx.doi.org/10.1016/j.bpj.2012.12.047.
[32] K.A.H. Wildman, D.-K. Lee, A. Ramamoorthy, Mechanism of lipid bilayer disruption by the human antimicrobial peptide, LL-37, Biochemistry 42 (2003) 6545–6558, http://dx.doi.org/10.1021/bi0273563.
[33] H. Strahl, L.W. Hamoen, Membrane potential is important for bacterial cell division, Proc. Natl. Acad. Sci. U. S. A. 107 (2010) 12281–12286, http://dx.doi.org/10.1073/pnas.1005485107.
[34] A. Marquette, E.S. Salnikov, E. Glattard, C. Aisenbrey, B. Bechinger, Magainin 2-PGLa interactions in membranes - two peptides that exhibit synergistic enhancement of antimicrobial activity, Curr. Top. Med. Chem. 16 (2015) 65–75 http://www.ncbi.nlm.nih.gov/pubmed/26139118.
[35] F. Kawai, M. Shoda, R. Harashima, Y. Sadaie, H. Hara, K. Matsumoto, Cardiolipin domains in *Bacillus subtilis* marburg membranes, J. Bacteriol. 186 (2004) 1475–1483, http://dx.doi.org/10.1128/JB.186.5.1475.
[36] A.-R. Pogmore, K.H. Seistrup, H. Strahl, The Gram-positive model organism *Bacillus subtilis* does not form detectable cardiolipin-specific lipid domains, bioRxiv 44 (2017), http://dx.doi.org/10.1101/190306.
[37] N. Malanovic, K. Lohner, Antimicrobial Peptides Targeting Gram-positive Bacteria, (2016), http://dx.doi.org/10.3390/ph9030059.
[38] Y.Q. Xiong, K. Mukhopadhyay, M.R. Yeaman, J. Adler-Moore, A.S. Bayer, T. David, L. Angeles, Functional interrelationships between cell membrane and cell wall in antimicrobial peptide-mediated killing of *Staphylococcus aureus*, Antimicrob. Agents Chemother. 49 (2005) 3114–3121, http://dx.doi.org/10.1128/AAC.49.8.3114–3121.2005.
[39] C. Weidenmaier, A. Peschel, V.A.J. Kempf, N. Lucindo, M.R. Yeaman, A.S. Bayer, DltABCD- and MprF-mediated cell envelope modifications of *Staphylococcus aureus* confer resistance to platelet microbicidal proteins and contribute to virulence in a rabbit endocarditis model, Microbiology 73 (2005) 8033–8038, http://dx.doi.org/10.1128/IAI.73.12.8033–8038.2005.
[40] H. Nishi, H. Komatsuzawa, T. Fujiwara, N. McCallum, M. Sugai, Reduced content of lysyl-phosphatidylglycerol in the cytoplasmic membrane affects susceptibility to moenomycin, as well as vancomycin, gentamicin, and antimicrobial peptides, in *Staphylococcus aureus*, Antimicrob. Agents Chemother. 48 (2004) 4800–4807, http://dx.doi.org/10.1128/AAC.48.12.4800-4807.2004.
[41] U.L. Rajbhandary, D. Söll, Aminoacyl-tRNAs, the bacterial cell envelope, and antibiotics, Proc. Natl. Acad. Sci. U. S. A. 105 (2008) 5285–5286, http://dx.doi.org/10.1073/pnas.0801193105.
[42] A. Peschel, R.W. Jack, M. Otto, L.V. Collins, P. Staubitz, G. Nicholson, H. Kalbacher, W.F. Nieuwenhuizen, G. Jung, A. Tarkowski, K.P. van Kessel, J.A. van Strijp, *Staphylococcus aureus* resistance to human defensins and evasion of neutrophil killing via the novel virulence factor MprF is based on modification of membrane lipids with l-lysine, J. Exp. Med. 193 (2001) 1067–1076, http://dx.doi.org/10.1084/jem.193.9.1067.
[43] S.J. Yang, C.C. Nast, N.N. Mishra, M.R. Yeaman, P.D. Fey, A.S. Bayer, Cell wall thickening is not a universal accompaniment of the daptomycin nonsusceptibility phenotype in *Staphylococcus aureus*: evidence for multiple resistance mechanisms, Antimicrob. Agents Chemother. 54 (2010) 3079–3085, http://dx.doi.org/10.1128/AAC.00122-10.
[44] A.S. Bayer, N.N. Mishra, G. Sakoulas, P. Nonejuie, C.C. Nast, J. Pogliano, K.T. Chen, S.N. Ellison, M.R. Yeaman, S.J. Yanga, Heterogeneity of mprF sequences in methicillin-resistant *Staphylococcus aureus* clinical isolates: role in cross-resistance between daptomycin and host defense antimicrobial peptides, Antimicrob. Agents Chemother. 58 (2014) 7462–7467, http://dx.doi.org/10.1128/AAC.03422-14.
[45] L.I. Salzberg, J.D. Helmann, Phenotypic and transcriptomic characterization of *Bacillus subtilis* mutants with grossly altered membrane composition, J. Bacteriol. 190 (2008) 7797–7807, http://dx.doi.org/10.1128/JB.00720-08.
[46] T.O. Khatib, H. Stevenson, M.R. Yeaman, A.S. Bayer, A. Pokorny, Binding of daptomycin to anionic lipid vesicles is reduced in the presence of lysyl-phosphatidylglycerol, Antimicrob. Agents Chemother. 60 (2016) 5051–5053, http://dx.doi.org/10.1128/AAC.00744-16.
[47] S.J. Yang, N.N. Mishra, A. Rubio, A.S. Bayer, Causal role of single nucleotide polymorphisms within the mprF gene of *Staphylococcus aureus* in daptomycin resistance, Antimicrob. Agents Chemother. 57 (2013) 5658–5664, http://dx.doi.org/10.1128/AAC.01184-13.
[48] T.T. Tran, J.M. Munita, C.A. Arias, Mechanisms of drug resistance: daptomycin resistance, Ann. N. Y. Acad. Sci. 1354 (2015) 32–53, http://dx.doi.org/10.1111/nyas.12948.
[49] A.Y. Peleg, S. Miyakis, D.V. Ward, A.M. Earl, A. Rubio, D.R. Cameron, S. Pillai, R.C. Moellering, G.M. Eliopoulos, Whole genome characterization of the mechanisms of daptomycin resistance in clinical and laboratory derived isolates of *Staphylococcus aureus*, PLoS One 7 (2012), http://dx.doi.org/10.1371/journal.pone.0028316.
[50] M. Hashimoto, H. Takahashi, Y. Hara, H. Hara, K. Asai, Y. Sadaie, K. Matsumoto, Induction of extracytoplasmic function sigma factors in *Bacillus subtilis* cells with membranes of reduced phosphatidylglycerol content, Genes Genet. Syst. 84 (2009) 191–198, http://dx.doi.org/10.1266/ggs.84.191.
[51] A. Arouri, M. Dathe, A. Blume, Peptide induced demixing in PG/PE lipid mixtures: a mechanism for the specificity of antimicrobial peptides towards bacterial membranes? Biochim. Biophys. Acta Biomembr. 1788 (2009) 650–659, http://dx.doi.org/10.1016/j.bbamem.2008.11.022.
[52] S. Finger, A. Kerth, M. Dathe, A. Blume, The efficacy of trivalent cyclic hexapeptides to induce lipid clustering in PG/PE membranes correlates with their antimicrobial activity, Biochim. Biophys. Acta Biomembr. 1848 ((2015) 2998–3006, http://dx.doi.org/10.1016/j.bbamem.2015.09.012.
[53] S. Omardien, S. Brul, S.A.J. Zaat, Antimicrobial activity of cationic antimicrobial peptides against Gram-positives: current progress made in understanding the mode of action and the response of bacteria, Front. Cell Dev. Biol. 4 (2016) 1–16, http://dx.doi.org/10.3389/fcell.2016.00111.
[54] I. Barák, K. Muchová, The role of lipid domains in bacterial cell processes, Int. J. Mol. Sci. 14 (2013) 4050–4065, http://dx.doi.org/10.3390/ijms14024050.
[55] L.M. Hays, J.H. Crowe, W. Wolkers, S. Rudenko, Factors affecting leakage of trapped solutes from phospholipid vesicles during thermotropic phase transitions, Cryobiology 42 (2001) 88–102, http://dx.doi.org/10.1006/cryo.2001.2307.